Transmutation of Skyrmions to Half-Solitons Driven by the Nonlinear Optical Spin Hall Effect

H. Flayac,[1] D. D. Solnyshkov,[1] I. A. Shelykh,[2,3] and G. Malpuech[1]

[1]*Institut Pascal, PHOTON-N2, Clermont Université, Blaise Pascal University, CNRS, 24 avenue des Landais, 63177 Aubière Cedex, France*

[2]*Science Institute, University of Iceland, Dunhagi-3, IS-107 Reykjavik, Iceland*

[3]*Division of Physics and Applied Physics, Nanyang Technological University, Singapore 637371, Singapore*

(Received 5 June 2012; published 3 January 2013)

We show that the spin domains, generated in the linear optical spin Hall effect by the analog of spin-orbit interaction for exciton polaritons, are associated with the formation of a Skyrmion lattice. In the nonlinear regime, the spin anisotropy of the polariton-polariton interactions results in a spatial compression of the domains and in a transmutation of the Skyrmions into oblique half-solitons. This phase transition is associated with both the focusing of the spin currents and the emergence of a strongly anisotropic emission pattern.

DOI: 10.1103/PhysRevLett.110.016404 PACS numbers: 71.36.+c, 03.75.Mn, 71.35.Lk

Introduction.—The ultimate goal of spintronics is to replace charge currents by pure spin currents. The spin Hall effect is one of the key concepts in this research field, since it allows the formation of a spin current perpendicular to the electric current in the absence of an applied magnetic field. Originally proposed by Dyakonov and Perel' in 1971 [1] and rediscovered by Hirsch in 1999 [2], it is now attracting a lot of attention [3,4]. Basically, this effect originates from the electron's spin-orbit interaction that makes its scattering on impurities spin dependent. One of the most serious obstacles to the realization of spintronic devices is the dramatic role played by the processes of spin relaxation, inducing information losses. The optical counterpart of spintronics: spinoptronics, appears as a valuable alternative thanks to very long decoherence times [5]. Another advantage of spinoptronics is the possibility to use collective bosonic effects and nonlinearities similar to self-focusing and soliton formation in nonlinear optics [6,7] in order to control the flow of particles. This makes a parallel to the physics of interacting spinor atomic Bose-Einstein condensates in the presence of artificial non-Abelian gauge fields [8–10]. This domain demonstrated incredible richness in the past years with the description of new quantum phases showing unique topological features [11–13].

Spinoptronics based on spinor exciton-polaritons (polaritons) [5] combines all potential advantages of spintronics, nonlinear optics and Bose-Einstein condensate physics, and therefore appears ideal to create spin textures, spinor topological defects [14–16], intense spin-polarized signals and even effective magnetic charges [17–19]. Polaritons are hybrid two-dimensional (2D) exciton-photon quasiparticles appearing in planar microcavities and showing extended coherence [20] and a record nonlinearity mediated by their excitonic part [21,22]. An effective magnetic field, analog of the spin-orbit interaction is present in the plane of microcavities, provided by the so-called TE-TM splitting [5] of the polaritons modes. This feature gives birth to the optical spin Hall effect (OSHE) [23] which became a popular research topic [24–28]. The OSHE, however, remains a linear effect, which does not capitalize on the exceptional nonlinear optical response of the polariton system. As a result, the created spin currents are by nature relatively weak, and demonstrate an angular aperture of about 45°.

Polariton-polariton interactions are strongly spin anisotropic [29], which imposes spin-dependent nonlinearities [30–32], resulting in the formation of spinor topological excitations such as half-vortices [14–16] and half-solitons [19,33]. These objects are circularly polarized dips on a linearly polarized background, the density in the center being one half of that at infinity. They differ from the topological excitations in spin-isotropic condensates, which are Skyrmions [34], appearing as domains of circular polarization inversion, while the total density remains constant: the core of the vortex in one component is filled by the other component.

In this Letter, we describe the spectacular transition arising between the linear and nonlinear OSHE. In the linear regime, the spin domains generated by the interplay between the particle flux and the TE-TM effective field are carrying topological charges forming a Skyrmion lattice. The situation is analogical to the recent studies on trapped atomic condensates within in a synthetic non-Abelian gauge field [10] mimicking the spin orbit interaction, where Skyrmions appear spontaneously [35]. In the nonlinear regime, one observes a dramatic change of the polarization texture, the emission profile and the nature of the topological excitations that are transmuted. The spin domains are abruptly spatially compressed by the spin-anisotropic polariton-polariton interactions. The phase transition occurs when the healing length of the nonlinear polariton fluid becomes smaller than the size of the polarization domains. The Skyrmions created by the

spin-orbit-like interaction abruptly transform into oblique half-solitons, stabilized in turn by the interactions. Finally, the total emission profile switches from isotropic to strongly anisotropic, accompanied by a strong focusing of the spin currents. The connection between self-focusing and *bright* solitons is commonly found in nonlinear optics [7], while in our case the phenomenon is linked with the onset of dark solitons. Our effect can also be seen as a nonlinear analogue of the magneto-optical Kerr effect where the microcavity is regarded as an effective magnetic material.

Linear OSHE.—The original proposal for the OSHE [23] involved a local resonant injection of polaritons with a well-defined nonzero momentum and linear polarization within the disorder landscape of a 2D microcavity. The resulting coherent Rayleigh scattering allowed a homogeneous redistribution of polaritons on an elastic ring in k space. However, in modern microcavities the disorder tends to be strongly reduced and would anyway be screened by the particles' interactions in the nonlinear regime.

An alternative configuration that we propose is to use a blue detuned laser oriented perpendicular to the microcavity plane and focused to a small spot [26] giving a sufficient extension in momentum space to excite directly the 2D dispersion of cavity polaritons on a ring [see Figs. 1(a) and 1(b)]. The polaritons then propagate radially outwards

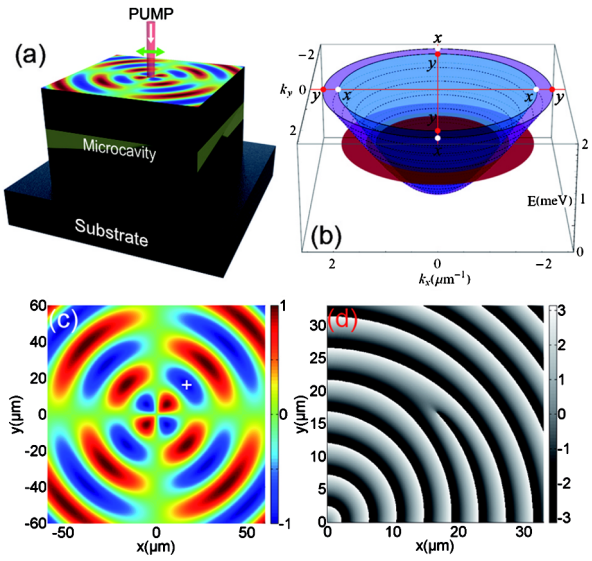

FIG. 1 (color online). (a) Scheme of the experiment with a cw tightly focused pump laser perpendicular to the cavity plane. (b) 2D dispersions of TE (purple or outer surface) and TM (blue or inner surface) polarized polaritons. Along the k_x (k_y) direction the TE mode is y (x) polarized and reciprocally for the TM mode. The red disk is the Fourier image of the pump laser (x polarized). (c) Degree of circular polarization ρ_c showing the antisymmetric circular polarization domains. (d) Zoom on the phase of the σ_+ component characterized by a forklike dislocation at the position of the density minimum [marked with a cross in (c)] which is the typical signature of a topological defect.

at a velocity fixed by the energy of the laser. The $\mathbf{k}$-dependent precession of the polariton pseudospin $\mathbf{S}$ around the effective magnetic field $\mathbf{H}_{\mathrm{LT}}$ associated with the TE-TM (or LT) splitting results in the appearance of alternating circularly polarized domains in the four quarters of the plane, as shown in Fig. 1(c).

For analytical considerations, let us begin with the idealized situation with particles continuously injected at $\mathbf{r} = \mathbf{0}$ with a well-defined energy $\hbar\omega_P$, linearly polarized along the x direction. This boundary condition excites an angle-dependent combination of the TE (t) and TM (l) eigenmodes assumed to have parabolic dispersions. The resulting stationary wave function $\boldsymbol{\psi}(r, \phi) = (\psi_+, \psi_-)^T$ reads (see Ref. [36])

$$\psi_+ = \sqrt{\frac{2N_0}{\pi k_0 r}} e^{-i\phi}[\cos\phi e^{ik_l r} + i\sin\phi e^{ik_t r}]e^{-r/r_0}, \quad (1)$$

$$\psi_- = \sqrt{\frac{2N_0}{\pi k_0 r}} e^{+i\phi}[\cos\phi e^{ik_l r} - i\sin\phi e^{ik_t r}]e^{-r/r_0}, \quad (2)$$

when written on the circular polarization (or spin ± 1) basis. Here, N_0 is the population imposed by the source at $r = 0$. $r_0 = \hbar k_0 \tau/m^*$ is a mean decay length where τ, m^* and $k_0 = (k_l + k_t)/2$ are the polariton lifetime, effective mass and mean excitation wave vector, respectively, with $k_{l,t} = \sqrt{2m_{l,t}\omega_P/\hbar}$. The distribution of the total density $n = n_+ + n_-$, $n_\pm = |\psi_\pm|^2$, is isotropic if one assumes a delta pump spot in real space populating equally the TE and TM branches in reciprocal space. Figure 1(b) shows the degree of circular polarization $\rho_c = (n_+ - n_-)/n$ of the polariton emission. It demonstrates the typical polarization oscillations with maxima appearing along diagonal directions [36], reproducing the polarization pattern of the original OSHE [23]. The positions of the maxima are given by

$$\phi = \frac{\pi}{4}, \quad \frac{5\pi}{4}: r_p^+ = \frac{(2p-1)\pi}{2(k_t - k_l)}, \quad r_p^- = \frac{p\pi}{k_t - k_l}, \quad (3)$$

$$\phi = \frac{3\pi}{4}, \quad \frac{7\pi}{4}: r_p^+ = \frac{p\pi}{k_t - k_l}, \quad r_p^- = \frac{(2p-1)\pi}{2(k_t - k_l)}, \quad (4)$$

where $p \in \mathbb{Z}^*$. A fundamental feature is that the cores of the spin domains are characterized by phase singularities in the circular polarized components shown in Fig. 1(d). They appear because the $\mathbf{H}_{\mathrm{LT}}$ projections on the x axis are exactly opposite on the two sides of the diagonal directions $\phi = (2p+1)\pi/4$, inducing a π phase difference after a half-period of pseudospin precession. This is the time reversal of the half-vortex unwinding scheme proposed in Ref. [37], which in our case produces a Skyrmion instead of a half-vortex, characterized by a homogeneous total density distribution. It appears because the *spin-anisotropic* interactions are absent and the effective magnetic field term [see Eq. (5)] is spin isotropic. The size of the

Skyrmions is governed radially by the quantity $\xi_r = \pi/(k_t - k_l)$ and tangentially by $\xi_t = r\pi/4$ imposed, respectively, by the strength and the geometry of $\mathbf{H}_{\mathrm{LT}}$.

Nonlinear OSHE.—When the density is increased, the quantum fluid gains nonlinearities and can accommodate excitations driven by the particle self-interactions. Skyrmions are transmuted into half-solitons whose size is governed this time by the healing length $\xi = \hbar/\sqrt{m^*\alpha n}$ of the nonlinear fluid. Qualitatively, one can expect the transition to occur when ξ becomes smaller than ξ_r which means that the interaction energy is dominating over the magnetic energy term. Once transformed, the resulting defect starts to feel the effective magnetic force provided by the $\mathbf{H}_{\mathrm{LT}}$, which now acts as a perturbation close to the pump spot.

The system of resonantly injected polaritons is accurately modeled with a system of dissipative equations for the coupled photonic $\varphi(\mathbf{r}, t)$ and excitonic fields $\chi(\mathbf{r}, t)$, each of which has two spin components [32]:

$$i\hbar\frac{\partial\varphi_\pm}{\partial t} = -\frac{\hbar^2}{2m_\varphi}\Delta\varphi_\pm + \Omega_R\chi_\pm + \beta\left(\frac{\partial}{\partial x} \mp i\frac{\partial}{\partial y}\right)^2\varphi_\mp + P_\pm e^{-i\omega_P t} - \frac{i\hbar}{2\tau_\varphi}\varphi_\pm, \tag{5}$$

$$i\hbar\frac{\partial\chi_\pm}{\partial t} = -\frac{\hbar^2}{2m_\chi}\Delta\chi_\pm + \Omega_R\varphi_\pm + (\alpha_1|\chi_\pm|^2 + \alpha_2|\chi_\mp|^2)\chi_\pm - \frac{i\hbar}{2\tau_\chi}\chi_\pm. \tag{6}$$

In the above expressions $\Omega_R = 5$ meV denotes the Rabi splitting coupling excitonic and photonic fields, $\tau_\chi = 400$ ps and $\tau_\varphi = 10$ ps are the lifetimes of excitons and photons, respectively, $P_\pm(\mathbf{r}, t)$ is a Gaussian with a 2 μm standard deviation, quasiresonant and linearly polarized (along the x axis: $P_+ = P_-$) optical pump having an energy $\hbar\omega_P$ blue detuned by $+1$ meV from the lower polariton branch at $\mathbf{k} = \mathbf{0}$. $m_\chi = 0.4m_0$, $m_\varphi = 5\times10^{-5}m_0$ are the effective masses of the excitons and cavity photons respectively (m_0 is the electron mass). The constant $\beta = \hbar^2/4(1/m_\varphi^l - 1/m_\varphi^t)$, where $m_\varphi^t = m_\varphi$ and $m_\varphi^l = 0.95m_\varphi$ are the effective masses of the photonic TE and TM modes, is the magnitude of the photonic TE-TM splitting. The corresponding terms give rise to the in-plane effective magnetic field $\mathbf{H}_{LT}(\mathbf{k})$. The constants $\alpha_1 = 6\times10^{-3}$ meV μm^2 and $\alpha_2 = -0.2\alpha_1$ describe the exciton-exciton interactions. All these parameters are typical for modern GaAs based microcavities.

The numerical results are presented in Fig. 2: Panels (a) and (e) show the circular polarization degree in the linear and nonlinear regimes, correspondingly. In the linear regime one can notice that the spin pattern is not symmetric, with the spin domains being slightly shifted towards the y axis as compared to Fig. 1(c). Indeed, in a realistic simulation (and in experiment) the use of a small size, monochromatic laser tends to excite TE and TM modes with two different wave vectors instead of two different energies as assumed in the original OSHE. This induces two different velocities and decay lengths for the TE and TM waves, slightly shifting in panel (c) the directions of maximum

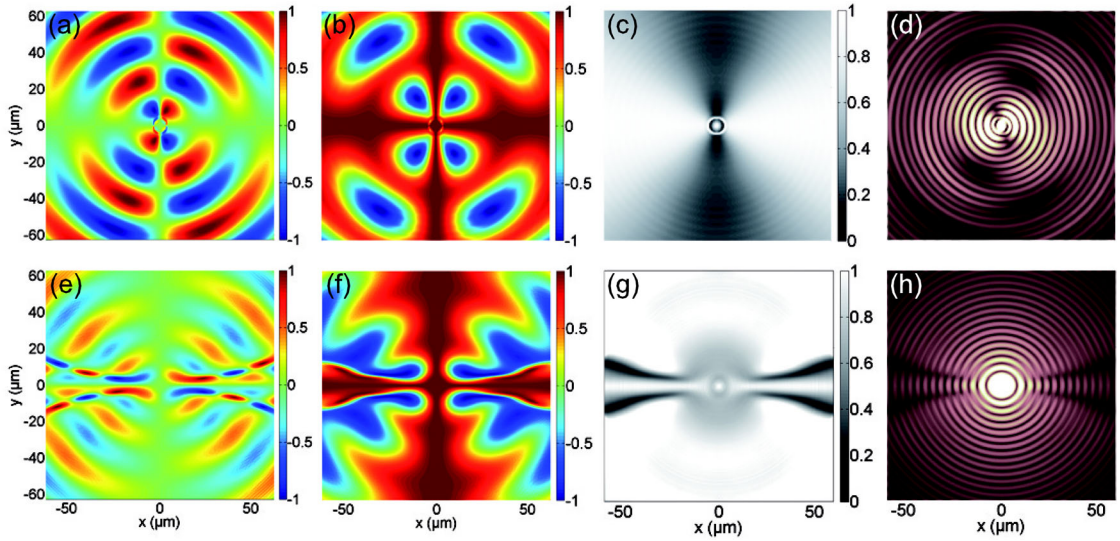

FIG. 2 (color online). (a)–(d) Linear and (e)–(h) nonlinear regimes. (a), (e) Degree of circular polarization showing (e) the compressed domains and the half-soliton formation at much larger density ($\alpha_1 n \simeq 1.5$ meV) than in panel (a) where $\alpha_1 n \simeq 0$. (b), (f) Degree of linear polarization $\rho_l = \Re(\phi_+\phi_-^*)/(n_+ + n_-)$. (b) the linear polarization oscillates in the oblique directions. (f) The half-solitons are evidenced as domain walls between x (red or light gray) and y (blue or dark gray) polarizations. (c), (g) Total emission, normalized to compensate for the decay, that goes from almost homogeneous (c) to the appearance of visible minima at the position of the half-solitons. (d), (h) Interference patterns with a circular plane wave: (d) typical forklike dislocations of Skyrmions in the σ_+ component and (h) elongated phase slip evidencing the half-solitons in the *global* phase.

circular polarization away from the diagonal direction, impacting on homogeneous distribution of the total intensity. This effect could be compensated by the use of an elliptic spot. As soon as the polariton density increases, the nonlinear effects start to dominate over the TE-TM splitting, and the interplay between the two leads to the transmutation of Skyrmions into half-solitons. The latter are characterized by phase dislocations visible close to the x axis in panel (h). They also appear in panel (f) as domain walls between x and y polarizations [33] and in panel (g) as sharp minima in the total density distribution. The angular dependence of the emission is therefore switching from smooth to strongly anisotropic. Interestingly, one can see in (e) an oscillation of the circular polarization along the half-soliton trajectory. Indeed, the decay of the total density far from the pump spot makes the half-solitons unstable against the effective field $\mathbf{H}_{\mathrm{LT}}$ as soon as it exceeds the density-dependent critical field $H_c = (\alpha_1 - \alpha_2)n/4$ [17]. This leads to spatial oscillations of the circular polarization degree of the solitons' cores. This is why we show in the panel (h) the phase associated with the *total* emission.

The transition between the linear and the nonlinear regime is analyzed in the Fig. 3(a), which shows the angular aperture $\Delta\alpha$ of the topological defects (solid purple line) and their local contribution to the total density $n_{\mathrm{rel}} = 1 - n_\varphi^{\pm}/(n_\varphi^{+} + n_\varphi^{-})$ (dashed blue line) as a function of the injected density n_0. The two curves show an abrupt switching, demonstrating a phase transition. $\Delta\alpha$ drops from 45° (Skyrmion) to less than 5° (half-soliton), whereas the total density minimum at the core of the topological defects rises from 0 to almost 0.5, the maximum possible value for a half-integer topological defect. The critical polariton density at which the transmutation occurs is consistent with the qualitative criterion: the healing length $\xi \sim \hbar/\sqrt{\alpha_1 n_\chi m_\varphi}$ becomes smaller than the Skyrmion size $r_0^{\pm}$.

The *compression* of the spin domains can be also be partly described in the framework of the pseudospin dynamics solely [5], which cannot address, however, the formation and dynamics of topological defects, but will allow us, by comparison with the full model, to quantify the impact of the transmutation on the spin pattern. The pseudospin precession equation reads $\partial_t \mathbf{S} = \mathbf{H} \times \mathbf{S}/\hbar$. The total effective magnetic field $\mathbf{H}$ represents the sum of the in-plane field $\mathbf{H}_{\mathrm{LT}}$ and of the nonlinear effective field provided by polariton spin anisotropy [5], normal to the cavity plane and describing the splitting between the circular polarized polariton states (intrinsic Zeeman splitting): $\mathbf{H}_Z = -(\alpha_1 - \alpha_2)(n_+ - n_-)/2\mathbf{u}_z$ [36]. The resulting system of nonlinear differential equations cannot be solved analytically in the general case.

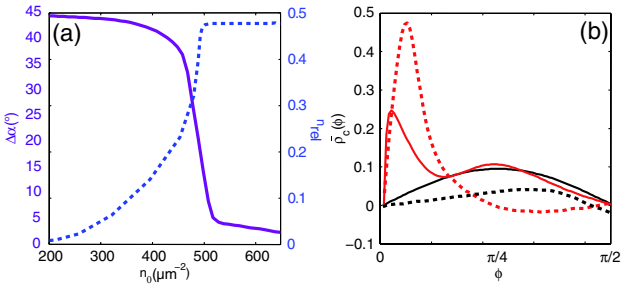

FIG. 3 (color online). (a) Phase transition: angular extension of the topological defects $\Delta\alpha$ (solid purple line, left scale) and their relative contribution to the total density n_{rel} (dashed blue line, right scale). (b) Focusing of the spin currents: Analytical (solid lines) vs numerical results (dashed lines). Black (red) curves: spatially integrated degree of circular polarization $\bar{\rho}_c$ in the linear (nonlinear) regime.

If the pseudospin is initially aligned along the x axis ($\mathbf{S} = S_x\mathbf{u}_x$), important conclusions can be made from the dynamics at short times. Indeed, if considering the dynamics of the S_y pseudospin projection, it turns out that the *contributions* of $\mathbf{H}_{\mathrm{LT}}$ and $\mathbf{H}_Z$ to this projection are able to cancel each other if the propagation direction at angle ϕ verifies the condition $H_0\cos(2\phi) = \alpha_1 n$. This compensation determines the direction of the maximal oscillations of the polarization degree (the focusing direction): instead of simply precessing around $\mathbf{H}_{\mathrm{LT}}$, the pseudospin turns further and further towards the z axis, because its S_y projection remains zero. In the linear case, this direction corresponds to the $\mathbf{H}_{\mathrm{LT}}$ completely orthogonal to the initial pseudospin $\phi = p\pi/4$, while in the nonlinear case the maximum is shifted towards the x axis [38]. This mechanism, being induced by the *intrinsic* Zeeman splitting, can therefore be seen as a nonlinear self-focusing effect analogue to what is observed in Kerr media [7], where it is induced by the intrinsic electric field of the beam.

The focusing of the spin currents is illustrated in Fig. 3(b) showing the analytical (from the previous short time reasoning) (solid lines) and numerical (dashed lines) space-integrated degree of circular polarization $\bar{\rho}_c(\phi)$. A substantial compression of the spin domains is obtained. In the linear regime (black lines) we see that the spin currents are hardly usable, while in the nonlinear regime (red lines) the self-focusing opens promising spin current generator perspectives. The effect is reduced in the simplified analytical case as compared to solutions of Eqs. (5) and (6) which encompass the formation of topological defects.

Finally we make the following remark: The Skyrmion is composed of a vortex component carrying a phase singularity an then a topological charge. However, in spinor fluids the topological charge is in general not conserved, because the superfluid velocity cannot be uniquely defined [37,39]. It can thus be removed by a continuous transformation, which is precisely what happens in our case during the transmutation into the *oblique half-soliton*, which is characterized by a smooth phase shift [19].

Conclusions.—In summary, we have demonstrated that the optical spin Hall effect is associated with the

formation of a Skyrmion lattice. In the nonlinear regime, a transmutation towards oblique half-solitons occurs. The latter are associated with the breaking of the cylindrical symmetry of the total density and a strong self-focusing of the spin currents in real space.

We would like to thank M. Glazov, H. Terças, and T. C. H. Liew for fruitful discussions. We acknowledge the support of the joint ANR QUANDYDE project, FP7 ITN SPINOPTRONICS (237252), and IRSES "POLAPHEN" (246912) project. I. A. S. benefited from the Rannis "Center of Excellence in polaritonics" and the IRSES "SPINMET" project.

[1] M. I. Dyakonov and V. I. Perel, Sov. Phys. JETP **13**, 467 (1971).
[2] J. E. Hirsch, Phys. Rev. Lett. **83**, 1834 (1999).
[3] S. Murakami, N. Nagaosa, and S.-C. Zhang, Science **301**, 1348 (2003).
[4] Y. K. Kato *et al.*, Science **306**, 1910 (2004).
[5] I. A. Shelykh, A. V. Kavokin, Y. G. Rubo, T. C. H. Liew, and G. Malpuech, Semicond. Sci. Technol. **25**, 013001 (2010).
[6] V. E. Zakharov and A. B. Shabat, Sov. Phys. JETP **34**, 62 (1972).
[7] Y. S. Kivshar and G. P. Agrawal, *Optical Solitons: From Fibers to Photonic Crystals* (Elsevier, New York, 2003).
[8] Y.-J. Lin, R. L. Compton, K. Jiménez-García, J. V. Porto, and I. B. Spielman, Nature (London) **462**, 628 (2009).
[9] Y.-J. Lin, K. Jiménez-García, and I. B. Spielman, Nature (London) **471**, 83 (2011).
[10] J. Dalibard, F. Gerbier, G. Juzeliunas, and P. Ohberg, Rev. Mod. Phys. **83**, 1523 (2011).
[11] X.-Q. Xu and J. H. Han, Phys. Rev. Lett. **108**, 185301 (2012).
[12] T. Kawakami, T. Mizushima, M. Nitta, and K. Machida, Phys. Rev. Lett. **109**, 015301 (2012).
[13] C. Wang, C. Gao, C.-M. Jian, and H. Zhai, Phys. Rev. Lett. **105**, 160403 (2010).
[14] G. E. Volovik, *The Universe in a He-Droplet* (Oxford University Press, New York, 2003).
[15] Y. G. Rubo, Phys. Rev. Lett. **99**, 106401 (2007).
[16] K. G. Lagoudakis, T. Ostatnicky, A. V. Kavokin, Y. G. Rubo, R. Andre, and B. Deveaud-Pledran, Science **326**, 974 (2009).
[17] D. D. Solnyshkov, H. Flayac, and G. Malpuech, Phys. Rev. B **85**, 073105 (2012).
[18] H. Flayac, D. D. Solnyshkov, and G. Malpuech, New J. Phys. **14**, 085018 (2012).
[19] R. Hivet *et al.*, Nat. Phys. **8**, 724 (2012).
[20] E. Wertz, *et al.*, Nat. Phys. **6**, 860 (2010).
[21] P. G. Savvidis, J. Baumberg, R. Stevenson, M. Skolnick, D. Whittaker, and J. Roberts, Phys. Rev. Lett. **84**, 1547 (2000).
[22] A. Baas, J. Ph. Karr, M. Romanelli, A. Bramati, and E. Giacobino, Phys. Rev. B **70**, 161307(R) (2004).
[23] A. Kavokin, G. Malpuech, and M. Glazov, Phys. Rev. Lett. **95**, 136601 (2005).
[24] E. Kammann, T. Liew, H. Ohadi, P. Cilibrizzi, P. Tsotsis, Z. Hatzopoulos, P. Savvidis, A. Kavokin, and P. Lagoudakis, Phys. Rev. Lett. **109**, 036404 (2012).
[25] C. Leyder, M. Romanelli, J. P. Karr, E. Giacobino, T. C. H. Liew, M. M. Glazov, A. V. Kavokin, G. Malpuech, and A. Bramati, Nat. Phys. **3**, 628 (2007).
[26] W. Langbein, I. Shelykh, D. Solnyshkov, G. Malpuech, Y. Rubo, and A. Kavokin, Phys. Rev. B **75**, 075323 (2007).
[27] M. Maragkou, C. E. Richards, T. Ostatnický, A. J. D. Grundy, J. Zajac, M. Hugues, W. Langbein, and P. G. Lagoudakis, Opt. Lett. **36**, 1095 (2011).
[28] A. Amo, T. Liew, C. Adrados, E. Giacobino, A. Kavokin, and A. Bramati, Phys. Rev. B **80**, 165325 (2009).
[29] P. Renucci, T. Amand, X. Marie, P. Senellart, J. Bloch, B. Sermage, and K. Kavokin, Phys. Rev. B **72**, 075317 (2005).
[30] N. Gippius, I. Shelykh, D. Solnyshkov, S. Gavrilov, Y. Rubo, A. Kavokin, S. Tikhodeev, and G. Malpuech, Phys. Rev. Lett. **98**, 236401 (2007).
[31] T. K. Paraïso, M. Wouters, Y. Léger, F. Morier-Genoud, and B. Deveaud-Plédran, Nat. Mater. **9**, 655 (2010).
[32] I. A. Shelykh, Y. G. Rubo, G. Malpuech, D. D. Solnyshkov, and A. Kavokin, Phys. Rev. Lett. **97**, 066402 (2006).
[33] H. Flayac, D. D. Solnyshkov, and G. Malpuech, Phys. Rev. B **83**, 193305 (2011).
[34] K. Kasamatsu, M. Tsubota, and M. Ueda, Phys. Rev. A **71**, 043611 (2005).
[35] H. Hu, B. Ramachandhran, H. Pu, and X. J. Liu, Phys. Rev. Lett. **108**, 010402 (2012).
[36] See Supplemental Material at http://link.aps.org/supplemental/10.1103/PhysRevLett.110.016404 for more details.
[37] M. R. Matthews, B. Anderson, P. Haljan, D. Hall, M. Holland, J. Williams, C. Wieman, and E. Cornell, Phys. Rev. Lett. **83**, 3358 (1999).
[38] See Supplemental Material at http://link.aps.org/supplemental/10.1103/PhysRevLett.110.016404 for a movie.
[39] A. J. Leggett, *Quantum Liquids* (Oxford University Press, Oxford, 2008), p. 154.